Defense Technical Information Center Compilation Part Notice

ADP011529

TITLE: Formation of Profiled Holographic Diffraction Gratings Using Physicochemical Interaction in As2Se3-Ag System

DISTRIBUTION: Approved for public release, distribution unlimited

This paper is part of the following report:

TITLE: International Workshop on Amorphous and Nanostructured Chalcogenides 1st, Fundamentals and Applications held in Bucharest, Romania, 25-28 Jun 2001. Part 1

To order the complete compilation report, use: ADA398590

The following component part numbers comprise the compilation report:
ADP011500 thru ADP011563

Journal of Optoelectronics and Advanced Materials Vol. 3, No. 2, June 2001, p. 383 - 388

FORMATION OF PROFILED HOLOGRAPHIC DIFFRACTION GRATINGS USING PHYSICOCHEMICAL INTERACTION IN As_2Se_3-Ag SYSTEM

M. V. Sopinskyy, P. F. Romanenko, I. Z. Indutnyy, E. F. Venger

Institute of Semiconductor Physics, National Academy of Sciences of Ukraine, Kiev, 03028 Ukraine

The method of blazed holographic diffraction gratings fabrication by transformation of an original symmetric grating grooves into asymmetric ones using inclined vacuum deposition of silver and additional chemical etching have been developed. As photoresist material for gratings recording light-sensitive chalcogenide glassy As_2Se_3 layers were used. The shape of grating grooves was determined with an atomic force microscope. Angular and spectral dependencies of the diffraction efficiency of the gratings were found, and a relation between optical features and the grating surface pattern was analyzed.

(Received June 5, 2001; accepted June 11, 2001)

Keywords: Hologram, Diffraction gratings, As_2Se_3-Ag system, Chalcogenide films

1. Introduction

Profiled (blazed) gratings make it possible to concentrate energy in a given spectrum range. Of special interest are profiled holographic gratings (PHGs), since they combine the advantages of ruled gratings with those of conventional (unprofiled) holographic gratings (CHGs), namely, high diffraction efficiency in a given spectrum range and low level of light scattering. There are two methods of blazed grating production: recording of interference fringe fields in photoresist materials using special exposing techniques, or transformation of conventional holographic gratings with symmetrical grooves into triangular groove grating by ion etching or another additional treatments [1].

The recent trend in CHG technology is the use of light-sensitive chalcogenide glassy semiconductor (CGS) films [2-5]. Vacuum-evaporated layers of chalcogenide glasses (for example As_2Se_3, As_2S_3, or As-S-Se composition) have shown to be a good registering media for holographic relief pattern fabrication due to its high resolution, optical uniformity, sensitivity to the irradiation of available lasers and absence of shrinkage under treatment. Due to light-induced structure transformations, their solubility, particularly, in organic alkaline solvents, changes. Based on this effect, high-quality symmetric CHGs were obtained with spatial frequencies in the range of 600 to 3600 mm^{-1} and diffraction efficiencies up to 80% in polarized light [2-5].

One of today's problem in this field is the transformation of symmetric CGS-based CHGs into asymmetric ones. Publication [5] reports PHGs prepared by ion etching of symmetric CHGs formed on CGS films. The unique properties of CGS films allow for other, unusual, methods for transforming their surface pattern. In [6, 7], we developed a method of fabricating blazed holographic gratings. In this method, symmetric grooves of an original grating are made asymmetric by using additional oblique monochromatic or polychromatic irradiation and chemical etching of the irradiated grating.

In this work, we made an attempt to fabricate PHGs through interactions that take place when silver layers are vacuum-deposited onto CGS films. Ag-CGS interaction begins during deposition [8] and continues at a different rate (depending on a specific Ag-CGS system) after the deposition process is terminated [9]. The metal penetrates into the semiconductor to form a metal-enriched (to several tens of atomic percent) phase. This phase differs in properties from both the metal and the semiconductor [10, 11]. Profiling was accomplished by transforming original symmetric (unprofiled) gratings written on CGS films. Here, we took advantage of the fact that the etching selectivity for Ag-doped CGS films is much higher than the photoinduced selectivity.

In this work we used most sensitive As_2Se_3 layers and amine-based negative etching solution.

The rate of interaction between As_2Se_3 and Ag is one of the highest among CGS-Me systems: intense interaction proceeds both during and after deposition of the metal even at room temperature [9].

2. Experimental procedures

The original holographic gratings were produced as usually by recording of a stationary interference fringe field onto As_2Se_3 films (thickness of 800-1000 nm) deposited onto high-quality polished glass substrates by thermal vacuum evaporation. The interferential pattern was generated by a He-Ne laser (wavelength of 632.8 nm) using the holographic setup assembled by the wave-amplitude division method. The spatial frequency of the gratings was 600 mm^{-1} and radiant exposure was ~10^{-1} J/cm^2. After exposure, the samples were chemically treated in an amine-based alkaline solution to form a relief pattern.

The next step was profiling. A thin (1-10 nm) Ag layer was deposited on the gratings at a certain angle φ varying from 10° to 80° with respect to the normal to the grating. The grating was mounted in such a way that the flux of evaporated silver was directed normally to the grooves. Ag penetrates into the As_2Se_3 layer during and after deposition as a result of chemically and thermally stimulated diffusion to form a metal-enriched semiconductor layer (reaction product). The etch rate of Ag-doped CGS films in alkaline etchants is much lower than for undoped ones; therefore, in subsequent etching of the grating, the former served as a protective mask. Unprotected regions of the As_2Se_3 layer were etched off, and the grating grooves became asymmetric. Profiling was performed in the same amine-based etchant, which was used to pattern the original gratings.

To estimate the profiling effect, we recorded angular and spectral dependencies of the absolute diffraction efficiency η for the original and transformed gratings in the first diffraction order (η is defined as the ratio of the first-order diffraction intensity to the incident intensity). Prior to optical measurements, the original and profiled gratings were covered by a 100-nm-thick reflection aluminum film. Angular dependencies (β is the angle of light incident) of η were measured using He-Ne laser (β= 0°-80°). Spectral measurements were carried out using the setup close to the Littrow's autocollimation scheme; the angle between the incident and diffracted beams was about 8°, and the spectral range was 400-800 nm. Both the spectral and angular dependencies of η were measured for *s*- and *p*-polarized light (*E* is perpendicular and parallel to grooves, respectively), as well as for unpolarized light.

The surface pattern of the gratings was examined with a Dimension 3000 scanning probe microscope (Digital Instruments) in the AFM tapping mode.

3. Results and discussion

The geometric and diffraction properties of the as-prepared and profiled gratings show that the effect of profiling depends on many parameters: the groove profile of initial gratings (which, in its turn, depends on several parameters, as well), the angle of deposition and the amount of Ag deposited, time of Ag-As_2Se_3 interaction and additional etching. This allows us to assume that the properties of PHGs thus obtained can be varied in wide limits. On the other hand, it becomes difficult to estimate the relative contribution of the above factors to the PHG performance. In general, they can be subdivided into three groups: those associated with the CGS film (primarily its thickness and deposition rate), those that govern the fabrication of the symmetric grating, and those closely related to Ag-CGS interaction.

The first two have been much studied. Empiric experimental studies and numerical simulation of gratings recording in CGS-based inorganic resists have been performed [2, 3], These experiments and also the simulation of surface patterning suggest that not only the depth but also the shape of the pattern depends on the initial thickness of the layers, their properties, exposure conditions, etch time, and etchant selectivity. Holographic diffraction gratings with grooves of sinusoidal and cycloidal shapes have been obtained.

We performed experiments with gratings that had sinusoidal grooves, which are the most studied. Fig. 1 shows a typical AFM image of the original symmetric grating with a spatial frequency of 600 mm^{-1}. The depth of the grooves is h_0 = 150 nm; hence, the modulation depth h_0/d = 0.09 (the period of the grating is 1667 nm). The mean angle of inclination of the facets (facet angle) is -10°, the steepest being 15°. The spectral and angular dependencies of η of such gratings was symmetrical

(within the accuracy of measurement: 2% for angular and 5% for spectral measurements) when they were irradiated from opposite directions perpendicular to the grooves.

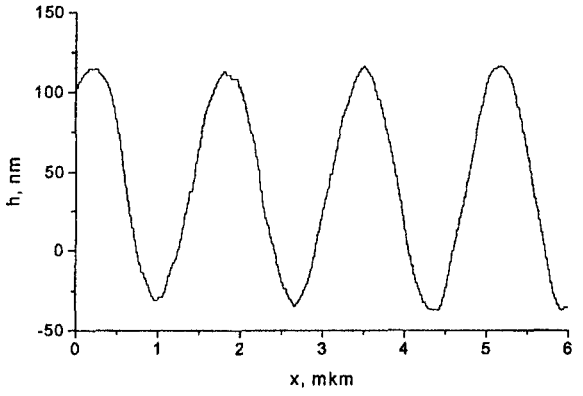

Fig. 1. Groove profile in the initial symmetric holographic grating.

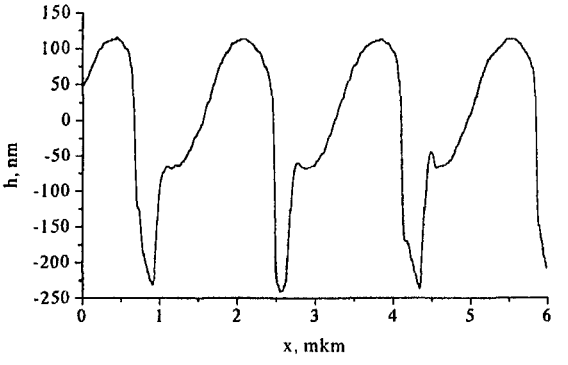

Fig. 2. Groove profile in the grating transformed from the initial grating shown in Fig. 1.

Fig. 2 shows the profile of a typical asymmetric grating made from a symmetric one by additional evaporation of a silver film of thickness $\{h_{Ag}\} = 3.6$ nm (this value is averaged over the grating area) at 50° to the normal to the substrate surface, and subsequent etching. The groove depth in the asymmetric grating is more than twice that in the initial one, 355 nm, and the modulation depth is $h_0/d \cong 0.21$. The minimum is 469 nm away from the left peak and 1198 nm from the right one; that is, the projection of the larger facet onto the substrate surface is nearly three-fourths of the grating period. The smaller facet has a gradually increasing steepness with an average angle of 37° with respect to the substrate. The larger facet can be divided into three parts: top (gently sloping), middle (nearly a plateau), and bottom (the steepest portion). The height of the gentle (top) portion somewhat exceeds the groove half-height; here, the average inclination is about 10°. The inclination of the bottom portion is close to the maximum steepness of the smaller facet. On average, the larger facet angle is about 16° with respect to the substrate.

From a comparison between the groove shapes of the initial and transformed gratings, it follows that the front facets of grooves of the initial grating (Ag were deposited onto these facets) remain practically intact after etching. This means that the reaction product nearly completely protected the CGS layer from dissolution during profiling etching. The first (gentle) portion of the larger slope virtually copies the profile of the initial sinusoidal grating. The back facets were affected by etching much more noticeably. Here, small plateaus correspond to the partially etched bottom part of the initial grating relief.

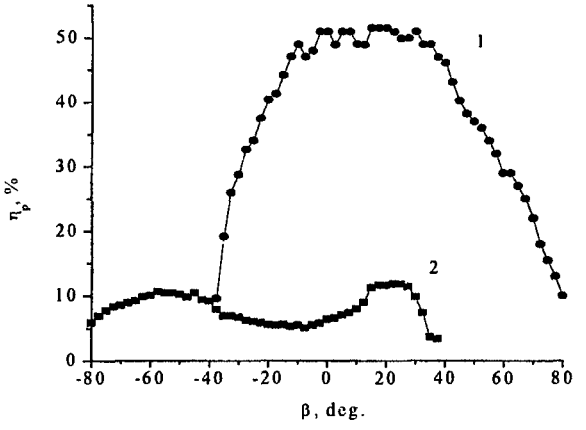

Fig. 3. Angular dependencies of the diffraction efficiency of the PHG for light polarized parallel to the groove direction. Wavelength is 632.8 nm.

The asymmetry of blazed grating is also displayed in angular and spectral dependencies of diffraction efficiency. For *p* polarization, the angular dependencies are plotted in Fig. 3. Here, curves 1 and 2 were obtained when light was incident on the larger and the smaller facet, respectively. For normal incidence ($\beta = 0$, symmetric arrangement of diffraction orders), the diffraction efficiencies measured on the two facets differ by a factor of 8.5. This points to the considerable asymmetry of the groove shape. For the larger facet, the maximum efficiency was observed when the angle of incidence was close to the mean facet angle. For the smaller one, two peaks appear: the angular position of one of them (-50°) is close to the mean slope of this facet, while that of the other (20°) coincides with the position of the peak from the larger facet and is likely to be associated with rereflections of the light incident on the larger facet. The share of total energy accounted for by conjugate diffraction orders is maximal at 20°; in other words, the maximum amount of light is reflected and rereflected at this angle.

For s-polarization we also obtained asymmetrical angular dependence but unlike *p* polarization, here distinct anomalies are observed. The anomaly at $\beta = 15°$ is associated with the disappearance (appearance) of the second order; while that at 38°, with the appearance (disappearance) of the conjugate order. The anomalies are more pronounced for the reflection from the smaller facet possibly because of the greater effect of the larger facet on the smaller than vice versa. Thus, the angular dependencies in the case of *p* polarization more adequately depict the groove shape.

Spectral dependencies of the diffraction efficiency for unpolarized light that were measured in the autocollimation regime for the blazed grating (curve 1 correspond to the bigger facet illumination, curve 2 – to that of the smaller facet), and for the symmetric grating (curve *3)* are shown in Fig. 4. Throughout the spectral range (400-800 nm), the diffraction efficiency for the larger facet exceeds that for the smaller one. For wavelengths of 620, 660, and 700 nm, these values differ by a factor of 5.7, 4.5, and 4.5, respectively. Also, the efficiency for the larger facet exceeds that for the symmetric grating, except for the short-wave part of the interval.

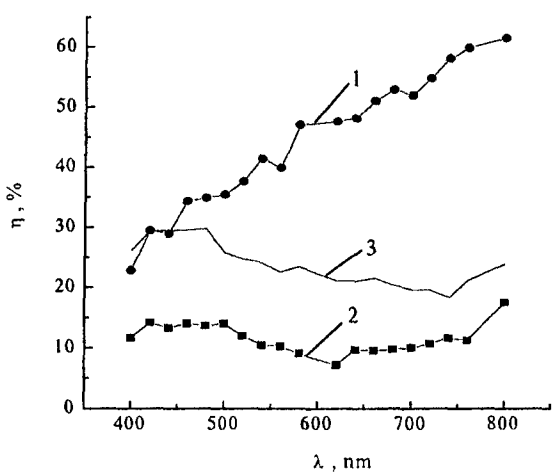

Fig. 4. Spectral dependencies of the diffraction efficiency for unpolarized light.

Simple geometric simulation of Ag deposition will allow us to describe Ag-As_2Se_3 interaction in quantitative terms. Let the *x* axis be directed normally to the grooves and the *y* axis, normally to the substrate (Fig. 5). The density of Ag deposited on the relief surface (and, hence, the thickness of the Ag film) depends on the amount of the metal evaporated and the angle between the Ag flux and each specific deposition area on the surface. Then, the thickness of the metal at a point *x* in the cross section perpendicular to the grating relief is given by

$$h_{Ag}(x) = K\cos\Theta(x), \quad (1)$$

where *K* is a proportionality coefficient, which depends on the amount of Ag deposited, and $\Theta(x)$ is the angle of incidence of the Ag flux on the groove surface at the point *x*.

We also have

$$\Theta(x) = \varphi - \alpha(x) \quad (2)$$

where φ is the angle of incidence of the Ag flux on the substrate that is reckoned from the normal to the substrate and $\alpha(x)$ is the groove inclination to the flat surface of the substrate at the point x.

Equation (1) is valid if the sticking coefficient of the metal is independent of the angle of incidence on the CGS film surface and on the amount of the metal deposited. The profile of the initial sinusoidal grating is described by the expression

$$h(x) = (h_0/2)(1 + \cos(2\pi x/d)), \quad (3)$$

where d is the grating period and h_0 is the height of the profile.

The inclination of this grating surface to the substrate surface is then expressed as

$$\alpha(x) = arctan\{[\pi h_0/d][-sin(2\pi x/d)]\}, \quad (4)$$

Fig. 5 illustrates the distribution of the Ag film thickness along the groove of the initial grating. The thickness was calculated by formulas (1), (2), and (4). Comparing this distribution with the distortions of the initial grating due to the metal deposition and subsequent etching, one can conclude that etching is virtually absent for $h_{Ag}(x) > 3$ nm. When $h_{Ag}(x)$ is less than 3 nm, the etch rate sharply grows. Since the Ag films (of thickness less than 10 nm) deposited on the noninteracting substrate are discontinuous (form islands), they could not serve as a protective mask during profiling etching. It appears that protection is provided by the top metal-doped CGS layer. The Ag thickness critical for the formation of the mask is seen to be about 3 nm. This value is close to that obtained earlier upon calculating the Ag amount incorporated into the As_2Se_3 film when the metal is thermally evaporated on this film [8]. The etch rate is maximal at the point one-fourth of the period away from the top of the groove back facet, where the Ag thickness estimated is minimal, 2.3 nm.

Using measurements of the groove shapes of the initial and profiled gratings, an empiric relationship $\Delta h(h_{Ag})$ can be derived, where Δh is the thickness of the As_2Se_3 film dissolved during etching and h_{Ag} is the amount of the Ag deposit. As follows from correlation analysis data, this empiric relationship is fairly accurately approximated by the sum of two exponentials:

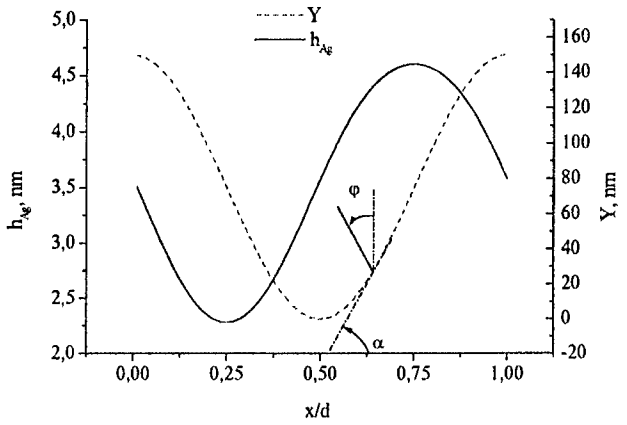

Fig. 5. Groove profile of the sinusoidal grating with $h_0 = 150$ nm and $d = 1667$ nm (Y, dashed line) and the distribution of the Ag deposit along this groove (h_{Ag}, solid line). The average thick-ness of the Ag layer is 3.6 nm.

$$\Delta h(h_{Ag}) = 204.93\exp\{-(h_{Ag} - 2.412)/0.125\} + 61.51\exp\{-(h_{Ag} - 2.412)/1.553\}, \quad (5)$$

With (5), we simulated the transformation of the initial symmetric gratings into asymmetric ones. The initial grating was assumed to be sinusoidal with a modulation depth of $h_0/d = 0.09$. Variable parameters were angle of vacuum deposition of Ag and the thickness of the metal deposited. Fig. 6 shows the results of numerical modeling for the angle of Ag deposition the same as for experimental grating onto Fig. 2, that is 50^0. Variable parameter here is the average thickness of the Ag layer: curve 1 – initial grating, curve 2 - the average thickness of deposited Ag is 4.18 nm, curve 3 – 4.02 nm, curve 4 – 3.86 nm.

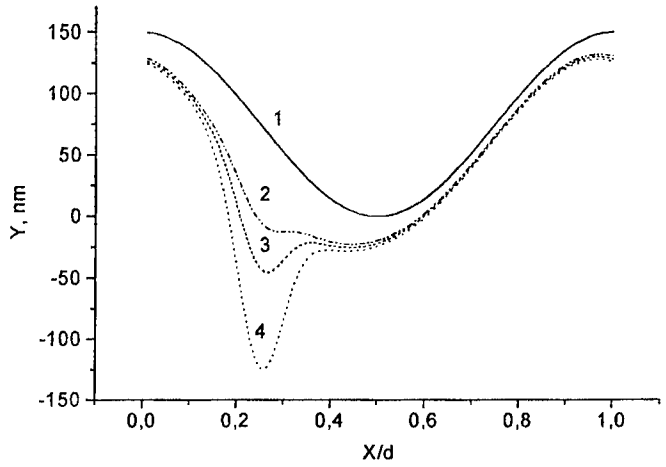

Fig. 6. Groove profile of initial grating (curve 1) and blazed gratings (curves 2, 3 and 4) obtained after Ag deposition and etching. Angle of deposition is equal 50^0.

We can see that as the Ag film gets thinner and etching of the Ag-doped grating becomes selective, the initially symmetric profile transforms into an asymmetric one because of a slight (-0.0*l*) shift of its maximum and a more considerable (-0.05*d*) shift of its minimum to the left of the initial grating grooves. The modulation depth remains practically unchanged in this case, since the minimum and maximum lower roughly equally. With further decreasing of Ag thickness, the groove shape can be approximated by an asymmetric trapezoid. The modulation depth in such a grating is somewhat larger than in the initial symmetric one. As Ag thickness continues to decrease, the groove shape becomes nearly triangular, the projections of the groove facets on the x axis being about $0.7d$ for the larger and $0.3d$ for the smaller. For an extremely thin Ag film, the larger facet has two drastically differing slopes because of a sharp increase in the etch rate. The maximum ratio of the facet projections is ~$0.72d/0.28d$ in this case.

4. Conclusion

The simple method of PHGs fabrication by additional treatment of initial gratings with symmetrical grooves have been developed. The blaze angle in the PHGs depends on the modulation depth of the initial sinusoidal gratings and also on the angle and the thickness of Ag deposition. The method enables recording of grating with designated blaze angle by changing the original grating formation parameters and the additional treatment conditions. The maximum value of absolute diffraction efficiency of obtained PHGs reached 60% for non-polarized light in the spectral range corresponded to a blaze angle.

References

[1] J. Flammand, F. Bonnemason, A. Thevenon, J. X. Lerner, Proc. SPIE **1055,** 288 (1989).
[2] I. Z. Indutnyi, I. I. Robur, P. F. Romanenko, A. V. Stronski, Proc. SPIE 1555, 248 (1991).
[3] I. Z. Indutnyi, A. V. Stronski, S. A. Kostioukevich. et al., Opt. Eng. 34, 1030(1995).
[4] R. R. Gerke, T. G. Dubrovina, P. A. Dmitrikov, M. D. Mikhailov, Opt. Zh. 64 (11), 26 (1997) [J. Opt. Technol. 64, 1008(1997)].
[5] A. V. Lukin, A. S. Makarov, F. A. Sattarov, et al., Opt. Zh. 66 (12), 73 (1999) [J. Opt. Technol. 66, 1071 (1999)].
[6] P. F. Romanenko, M. V. Sopinski, I. Z. Indvtnyi, Proc. SPIE 3573, 457(1998).
[7] P. F. Romanenko, N. V. SopinskiT, I. Z. Indutnyi, et al., Zh. Prikl. Spektrosk. 66 (4), 587 (1999).
[8] M. T. Kostyshin, V. L. Gromashevskii, N. V. Sopinskii, et al., Zh. Tekh. Fiz. 54 (6), 1231 (1984) [Sov. Phys. Tech. Phys. 29,709(1984)].
[9] I. Z. Indutnyi, M. T. Kostyshin, O. P. Kasyarum, et al., Photostlmulated Interactions in Metal-Semiconductor Structures (Naukova Dumka, Kiev, 1992).
[10] A. G. Fitzgerald, C. P. McHardy, Surf. Sci. 152/153, 1255(1985).
[11] V. Honig, V. Fedorov, G. Liebmann, P. Suptitz, Phys. Status Solidi A 96 (2), 611 (1986).
[12] P. F. Romanenko, I. I. Robur, A. V. Stronskii. Optoelektron. Poluprovodn. Tekh. 27, 47 (1994).
[13] M. C. Hutley, Diffraction Gratings (Academic, London, 1982).